AD-A120 939 DENSIFICATION OF MONOCLINIC ZRO2 WITH VANADATE ADDITIVES(U) ILLINOIS UNIV AT URBANA DEPT OF CERAMIC ENGINEERING R C BUCHANAN ET AL. 15 JUL 82 TR-4 1/1

UNCLASSIFIED N0004-78-C-0279 F/G 7/2 NL

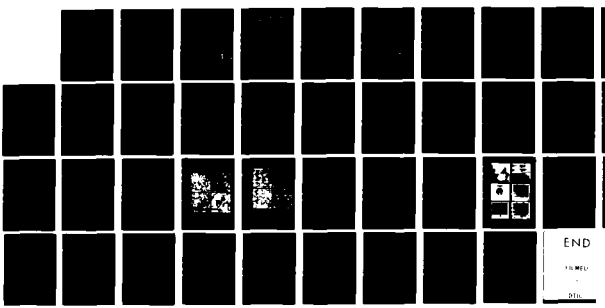

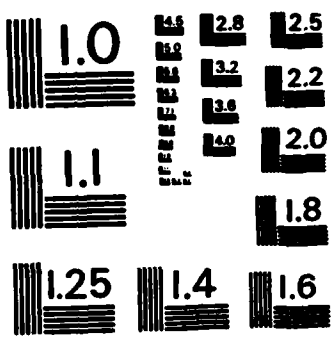

(12)

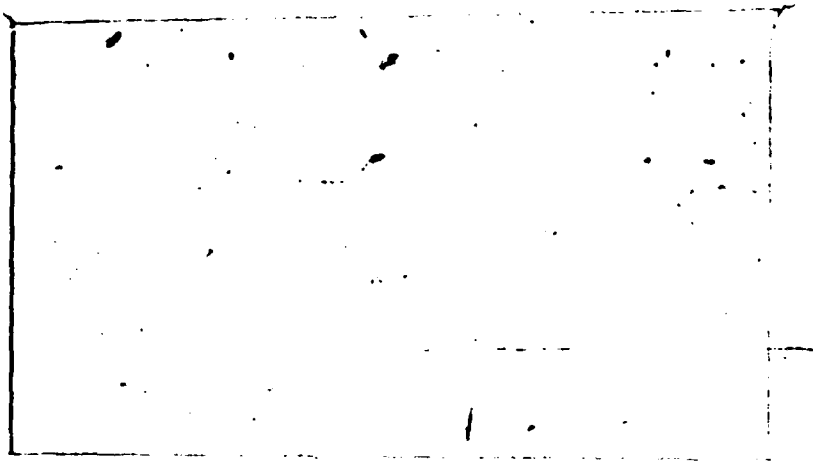

DEPARTMENT OF CERAMIC ENGINEERING

UNIVERSITY OF ILLINOIS

URBANA, ILLINOIS

Final Report
Technical Report No. 4
Contract No.: US NAVY-N-00014-78-C-0279

DENSIFICATION OF MONOCLINIC ZrO_2 WITH VANADATE ADDITIVES

by

R. C. Buchanan and H. D. DeFord

July 1982

Department of Ceramic Engineering
University of Illinois at Urbana-Champaign
Urbana, IL 61801

This research was supported by the Office of Naval Research,
Department of the Navy.
Contract No. US NAVY-N-00014-78-C-0279

SECURITY CLASSIFICATION OF THIS PAGE (When Data Entered)

REPORT DOCUMENTATION PAGE

READ INSTRUCTIONS BEFORE COMPLETING FORM

1. REPORT NUMBER: #4	2. GOVT ACCESSION NO.: AD-A120939
3. RECIPIENT'S CATALOG NUMBER	
4. TITLE (and Subtitle): Densification of ~~Zirconia with Borates~~ MONOCLINIC ZrO_2 WITH VANADATE ADDITIVES	5. TYPE OF REPORT & PERIOD COVERED: Interim Research Report March 1, 1979-March, 1982
	6. PERFORMING ORG. REPORT NUMBER
7. AUTHOR(s): R. C. Buchanan and D. E. DeFord	8. CONTRACT OR GRANT NUMBER(s): US NAVY N00014-78-C-0279
9. PERFORMING ORGANIZATION NAME AND ADDRESS: University of Illinois at Urbana-Champaign, Department of Ceramic Engineering, 105 S. Goodwin, Urbana, IL 61801	10. PROGRAM ELEMENT, PROJECT, TASK AREA & WORK UNIT NUMBERS: ONR-Metallurgy Code 471
11. CONTROLLING OFFICE NAME AND ADDRESS: Office of Naval Research, Metallurgy, 800 N. Quincy Ave., Arlington, VA 22217	12. REPORT DATE: 7-15-82
	13. NUMBER OF PAGES
14. MONITORING AGENCY NAME & ADDRESS (if different from Controlling Office): Same as control office	15. SECURITY CLASS. (of this report): Unclassified
	15a. DECLASSIFICATION/DOWNGRADING SCHEDULE

16. DISTRIBUTION STATEMENT (of this Report)

widespread; required numbers of copies to defence documentation center; individuals and organizations on approved distribution list furnished by Metallurgy and Ceramic Program--ONR

17. DISTRIBUTION STATEMENT (of the abstract entered in Block 20, if different from Report)

same

18. SUPPLEMENTARY NOTES

none

19. KEY WORDS (Continue on reverse side if necessary and identify by block number)

zirconium oxide-low temperature sintering with vanadium additives

20. ABSTRACT (Continue on reverse side if necessary and identify by block number)

Sintering of monoclinic ZrO_2 ceramic powders was carried out < 1150°C using 1-8 wt% V_2O_5 (or ZrV_2O_7 equivalent) as flux additive. Densities > 92% ThD were achieved using a relatively coarse commercial (PS ~ 1.5 μm) ZrO_2 powder with 1.5-2.0 wt% V_2O_5 additive by sintering in air at 1100°C for up to 24 h. High pressed densities were found to be correlated to high fired densities, thus ZrO_2 powders with average particle size < 1 μm gave lower densities.

DD FORM 1 JAN 73 1473 EDITION OF 1 NOV 65 IS OBSOLETE
S/N 0102-LF-014-6601

SECURITY CLASSIFICATION OF THIS PAGE (When Data Entered)

Microstructural and chemical analysis of the sintered samples were carried out to determine the composition and relative distribution of the ZrO_2 and intergranular phases. Methods used included: SEM, TEM, X-ray microanalysis (EDAX), EPR, DTA, TGA, and arc emission spectroscopy techniques. Results showed the solubility of vanadium in the ZrO_2 phase to be low (~ 0.2 at.%-indicated to be V^{4+} ions). The bulk of the added vanadium was found in the grain boundary region which together with Ca, Si, and Mg impurities formed the amorphous bonding phase. This indicates densification by reactive liquid phase sintering aided perhaps by defect migration. The optimum combination of density, strength, electrical conductivity, and expansion coefficient was found for a V_2O_5 content of 1.5 wt%.

Table of Contents

DENSIFICATION OF MONOCLINIC ZrO_2 WITH VANADATE ADDITIVES

by

R. C. Buchanan and H. D. DeFord

Abstract

Sintering of monoclinic ZrO_2 ceramic powders was carried out < 1150°C using 1-8 wt% V_2O_5 (or ZrV_2O_7 equivalent) as flux additive. Densities > 92% ThD were achieved using a relatively coarse commercial (PS ≈ 1.5 μm) ZrO_2 powder with 1.5-2.0 wt% V_2O_5 additive by sintering in air at 1100°C for up to 24 hr. High pressed densities were found to be correlated to high fired densities, thus ZrO_2 powders with average particle size < 1 μm gave lower densities.

Microstructural and chemical analysis of the sintered samples were carried out to determine the composition and relative distribution of the ZrO_2 and intergranular phases. Methods used included: SEM, TEM, X-ray microanalysis (EDAX), EPR, DTA, TGA, and arc emission spectroscopy techniques. Results showed the solubility of vanadium in the ZrO_2 phase to be low (≈ 0.2 at.%--indicated to be V^{4+} ions). The bulk of the added vanadium was found in the grain boundary region which together with Ca, Si, and Mg impurities formed the amorphous bonding phase. This indicates densification by reactive liquid phase sintering aided perhaps by defect migration. The optimum combination of density, strength, electrical conductivity, and expansion coefficient was found for a V_2O_5 content of 1.5 wt%.

DENSIFICATION OF MONOCLINIC ZrO_2 WITH VANADATE ADDITIVES

I. Introduction

Widespread use is made of zirconium dioxide as a refractory material for high temperature furnace applications and increasingly for solid electrolyte fuel cell and oxygen sensor applications. ZrO_2 exhibits three polymorphs, namely, the monoclinic, tetragonal, and cubic phases. The monoclinic phase is stable at room temperature but transforms to the tetragonal phase at ~ 1150°C (depending on purity, particle size, and heating rate) with a volume decrease of 4-5%. High densities for ZrO_2 can be obtained by sintering in air above 1700°C, but the volume expansion accompanying the transformation to the monoclinic phase on cooling results in microcracking and severe loss of strength. Use of the monoclinic ZrO_2 phase, therefore, would require that the material be sintered below the transformation range. In practice, the destructive transformation is avoided by use of the cubic stabilized phase, formed by solid solution with up to 15 mol% of such oxides as MgO, CaO, and Y_2O_3.[1,2] Presence of the CaO and Y_2O_3 additives increases the oxygen ion mobility and ionic conductivity of the ZrO_2, but precise control of the microstructure is difficult to achieve at these high temperatures. A significant reduction in the sintering temperatures would, therefore, allow for greater control of microstructure and second phases.

This research was initiated to develop a procedure for lowering the sintering temperature of unstabilized ZrO_2 (USZ) to below the monoclinic-tetragonal transformation temperature. This would allow the production of a dense, low expansion (~ 7 x 10^{-6}/°C for USZ) ceramic body

which could be used at temperatures below 1100°C for substrate and similar type applications.

Three methods have been commonly used to improve the sintering behavior of refractory oxides: 1) the use of fine, reactive powders (< 0.5 μm), 2) the use of low melting additives, and 3) hot-pressing. All three methods were evaluated; however, a high degree of densification below the transformation temperature was obtained only by liquid phase sintering.

The addition of a low melting second phase, in which the refractory phase is soluble, can result in a high degree of densification from particle rearrangement and solution-precipitation processes. Vanadium pentoxide (V_2O_5) was found to be a suitable additive for low temperature sintering. V_2O_5 forms a very fluid melt (< 5 P just above its melting point-690°C),[3] forms a eutectic with USZ at ~ 670°C,[4] takes USZ into solution,[5] and has been shown to enhance densification in other oxide systems by formation of a reactive liquid phase and the creation of lattice defects.[6-11]

The system ZrO_2-V_2O_5 itself has not been much studied. Peyronel[12] prepared the compound ZrV_2O_7 from an aqueous mixture of ammonium vanadate and zirconyl nitrate solutions and reported the structure to be cubic, melting incongruently at ~ 747°C to liquid and ZrO_2. More extensive phase studies by Burdese and Bolera[4] developed the phase diagram shown in Fig. 1. As indicated the only compound which exists in the system is ZrV_2O_7 and there is apparently little or no mutual solid solubility of either constituent. Work by King and Suber[13] and Cirilli, et al.[14] indicate that solid state formation of the compound from ZrO_2 and V_2O_5 takes place only slowly and with some difficulty between 600-800°C. Craig and Hummel,[15]

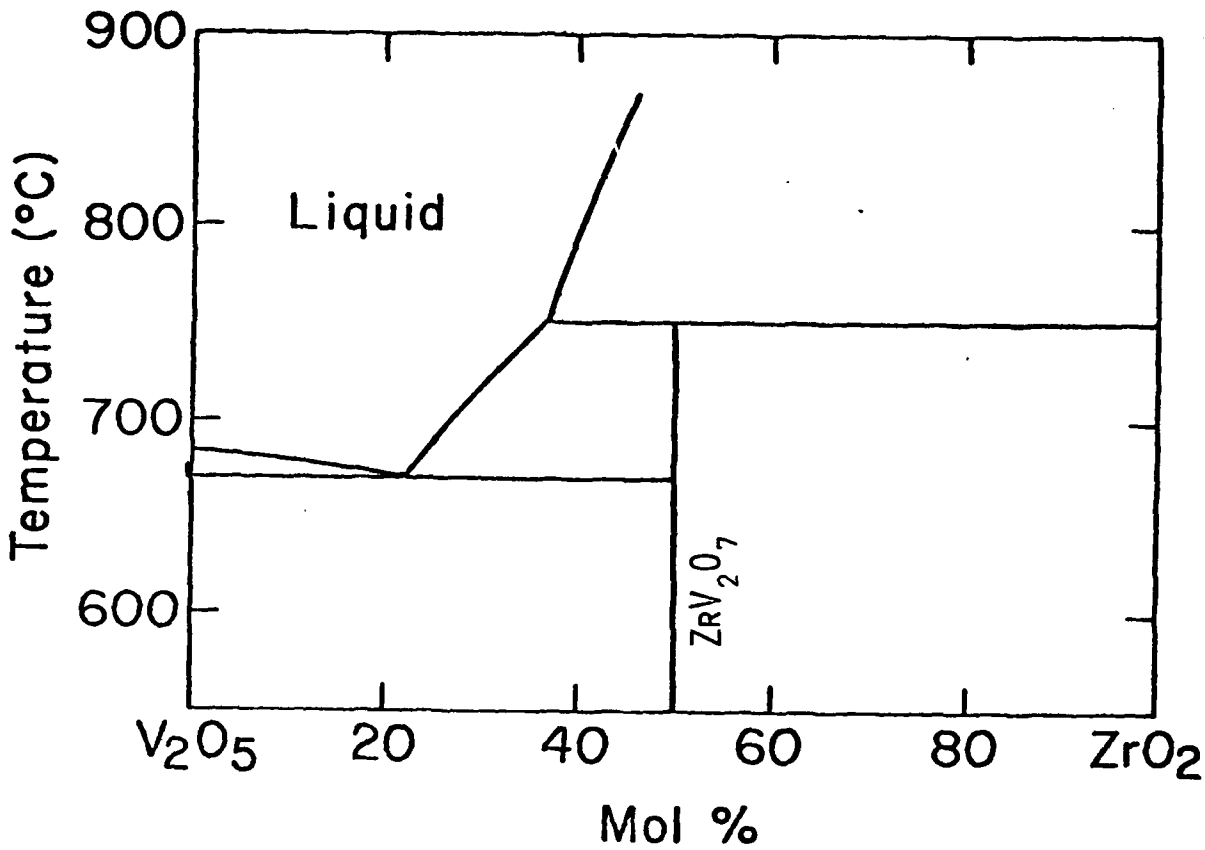

FIGURE 1. Phase diagram for ZrO_2-V_2O_5 system (Burdese and Bolera[4])

however, prepared the compound by successive heat treatments at 600° and 700°C for 100 h in a sealed platinum tube and confirmed the existence of the cubic structure.

One system of interest in which V_2O_5 exhibits catalytic behavior is the $ZrO-SiO_2-V_2O_5$ system. Additions of 2-30 wt% of V_2O_5 to equimolar mixtures of ZrO_2 and SiO_2 reduced the formation temperature for zircon ($ZrSiO_4$) from ~ 1350°C to as low as ~ 800°C. This is illustrated in Fig. 2 from the work of Bystrikov and Cherepanov.[16] Work by Demiray, et al.[17] and Matkovitch and Corbett,[18] indicate that ~ 2-4 wt% of the V_2O_5 went into solid solution in the structure during the formation of the zircon. The vanadium diffused into the lattice as V^{4+} ions, and according to Bystrikov,[19] this was possible only during the formation of zircon. Prolonged heating at temperatures in excess of 1000°C resulted in exsolution of V^{4+} from the zircon lattice, which could then be reoxidized to VO_2 or V_2O_5.

Dmitriev Semin, et al.[20] have suggested another mechanism for the observed accelerated effect of small amounts of V_2O_5 (~ 2 wt%) on phenacite (Be_2SiO_4) formation and on sintering in the system $BeO-SiO_2-V_2O_5$. Partial surface reduction of V_2O_5 to VO_2 and subsequent diffusion of V^{4+} into the host lattice was also noted for this system. A crucial condition for the solid state reactions to occur appeared to be the formation, with V_2O_5, of a low melting microeutectic surface phase around the particles to be sintered. This had the effect of reducing the activation energy for the reaction, and providing for faster diffusion of the reacting species. Melting of the eutectic phase was also found to accelerate the formation of phenacite.

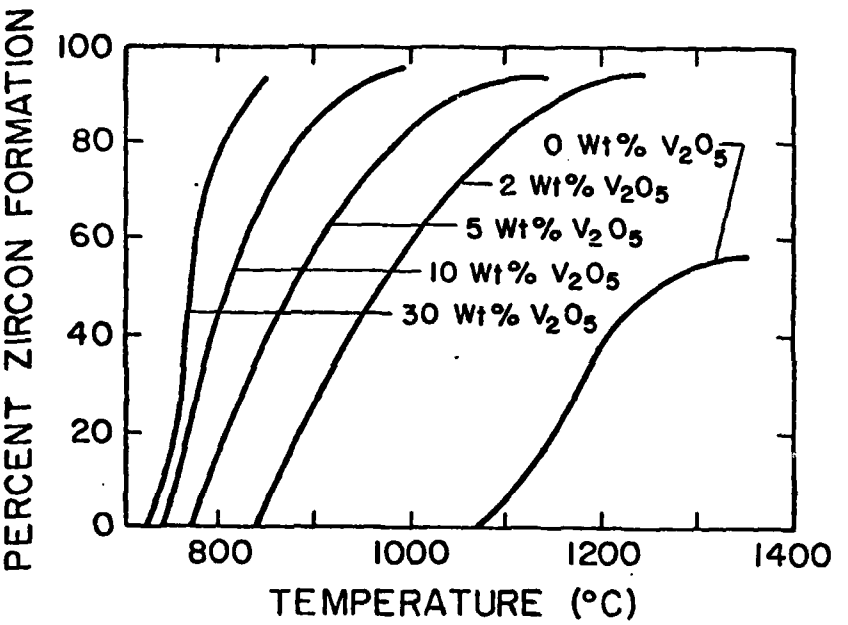

FIGURE 2. Accelerated formation of Zircon with V_2O_5 (after Bystrikov and Cherepanov[16])

This mechanism is similar to that postulated by Tacvorian[21] for the sintering of ThO_2 and similar refractory oxides at temperatures substantially below their melting points. The microeutectic phase may be produced during the sintering reaction or alternately be thoroughly dispersed on the particles prior to sintering. Thus for the ZrO-V_2O_5 system, the V_2O_5 could be added directly to the ZrO_2 powder, or a prereacted ZrV_2O_7 phase could be added as the sintering aid. Thus, the observed effectiveness of vanadate additives as a sintering aid appear from the discussion to be a complex reaction sequence requiring some or all of the following steps:

a. Complete coating of the particles to be sintered by the dispersed vanadate phase.

b. Formation on heating, of a low melting surface eutectic compound. This lowers the sintering activation energy.

c. Coalescence of the eutectic phase on further heating through solid state and surface migration of generated vacancies and diffusion of V^{4+} ions into the host lattice.

d. Liquid phase sintering by rearrangement and solution precipitation on melting of the eutectic phase.

The latter mechanism would be expected to be dominant. In addition to the aforementioned objectives, therefore, this study was aimed at developing and understanding the sintering mechanisms, process parameters and optimum composition to achieve dense fired monoclinic ZrO_2 bodies at temperatures below ~1150°C. Optimization of the mechanical, electrical and thermal stability characteristics of the sintered ZrO_2 bodies, analysis of the

microstructures and correlation of these to the densification mechanism(s) and properties, were also prime considerations.

Results given are for samples fired at 1100°C for 24 h, unless otherwise specified.

II. Experimental Procedure

Several unstabilized ZrO_2(USZ) powders were used in this investigation; USZ-1[a] (avg particle size 1.5 μm) was the most responsive of these powders, and is primarily reported on in this study.

Vanadium was added in the form of either the pentavalent oxide, V_2O_5[b] (avg ps < 0.5 μm), or as zirconium pyrovanadate, ZrV_2O_7 (avg ps < 0.5 μm), which was prepared by a precipitation procedure.[12] Both additives were essentially equivalent as sintering aids, but V_2O_5 was primarily used because of availability. Batches of ZrO_2 containing additions of 0-8 wt% V_2O_5 were weighed, wet-milled for 5 h in polypropylene jars containing dense ZrO_2 pellets in isopropanol, and were then air-dried followed by dry milling for 5 h.

Approximately 2 wt% binder[c] was added. The powders were then dried to ~ 3 wt% H_2O content, followed by granulation through a 35-mesh sieve. Sample discs ~ 1.6 cm in diameter and ~ 0.3 cm thick were formed at uniaxial pressures ranging from 34.5-345.0 MPa. Bulk green densities were determined from the calcined weights and measured dimensions of the pressed samples.

Some samples containing 2 wt% V_2O_5 were hot-pressed at 1025°C for 1.5 h

---

a) Zircoa A; Zirconia Corp. of America.
b) Fisher Certified; Fisher Scientific Co.
c) Carbowax 4000; Union Carbide Corp.

at 48 MPa. All other samples were sintered in a muffle furnace using SiC heating elements at 1100°C for up to 24 h on platinum sheets supported by ZrO_2 setter plates. Some exudation of the liquid phase, especially noticeable for V_2O_5 contents > 2.0 wt%, was observed for samples which were furnace cooled. Air-quenching of the samples eliminated the exudation, resulting in a homogeneous fired ceramic.

DTA, TGA, X-ray diffraction (XRD), and Hot-Stage XRD techniques were used to analyze the reactions and phase changes which occurred during the sintering cycle. Electron paramagnetic resonance (EPR) was used to determine the presence of V^{4+} ions in the fired samples. Arc emission spectroscopy was used to determine the approximate amount of vanadium which diffused into the ZrO_2 grains during sintering. The samples were repeatedly wet-milled and washed to remove the intergranular phase prior to analysis. Weight loss data was obtained from calcined samples which were weighed, fired at 1100°C for 24 h, and then reweighed. Fired densities were determined from the weights and geometric dimensions or by liquid displacement techniques.

A scanning electron microscope (SEM) equipped with an energy dispersive X-ray analyzer was used for microstructural analysis of polished and fractured sections of the fired samples. A transmission electron microscope (TEM) equipped with an energy dispersive X-ray analyzer was used for analysis of ion-milled samples.

DC electrical resistivity measurements were made up to 800°C using a shielded furnace and electrometer. Thermal expansion measurements up to 950°C were made with a quartz dilatometer. Tensile strengths of the fired samples were calculated from dimensions and failure loads of sample discs which were loaded diametrically (in compression) to failure. Sample discs

of high density Al_2O_3, for which the tensile and flexure strengths were known, were used to calibrate the system and obtain estimates of the flexural strengths of the fired ZrO_2 samples by comparison.

III. Results and Discussion

A. Processing and Characterization

Hot-stage X-ray diffraction (XRD) data collected at 1100° and 1150°C are shown in Fig. 3 for previously unfired ZrO_2 samples containing 0.0, 1.5, 2.0, and 8.0 wt% V_2O_5. In the region of 18° to 32° 2θ. The monoclinic phase was indicated by the presence of the monoclinic ($1\bar{1}1$) and (111) XRD peaks, and the tetragonal phase by the tetragonal (111) XRD peak. At 1100°C, only the ZrO_2 sample with no V_2O_5 contained the tetragonal phase. At 1150°C, all the samples contained some tetragonal phase, indicating that the optimum sintering temperature for samples containing V_2O_5 would be between 1100° and 1150°C. The ZrO_2 powder containing no V_2O_5 was completely transformed to the tetragonal phase at 1150°C, and the amount of tetragonal phase in the other samples steadily decreased as the V_2O_5 content was increased to 2 wt%. For additions > 2 wt%, the amount of tetragonal phase present at 1150°C was constant, indicating that the solid solubility limit of vanadium ions in the ZrO_2 lattice had been reached. This data essentially dictated the choice of 1100°C as the sintering temperature for the ZrO_2-V_2O_5 samples.

DTA heating (to 1100°C) and cooling curves of unfired ZrO_2 samples containing 0.0, 1.0, 1.5, and 2.0 wt% V_2O_5 are shown in Fig. 4. As indicated also by the hot-stage XRD data, heating of the ZrO_2 sample containing no V_2O_5 to 1100°C, resulted in partial transformation to the tetragonal phase, shown in Fig. 4 by the endotherm beginning at ~ 1040°C.

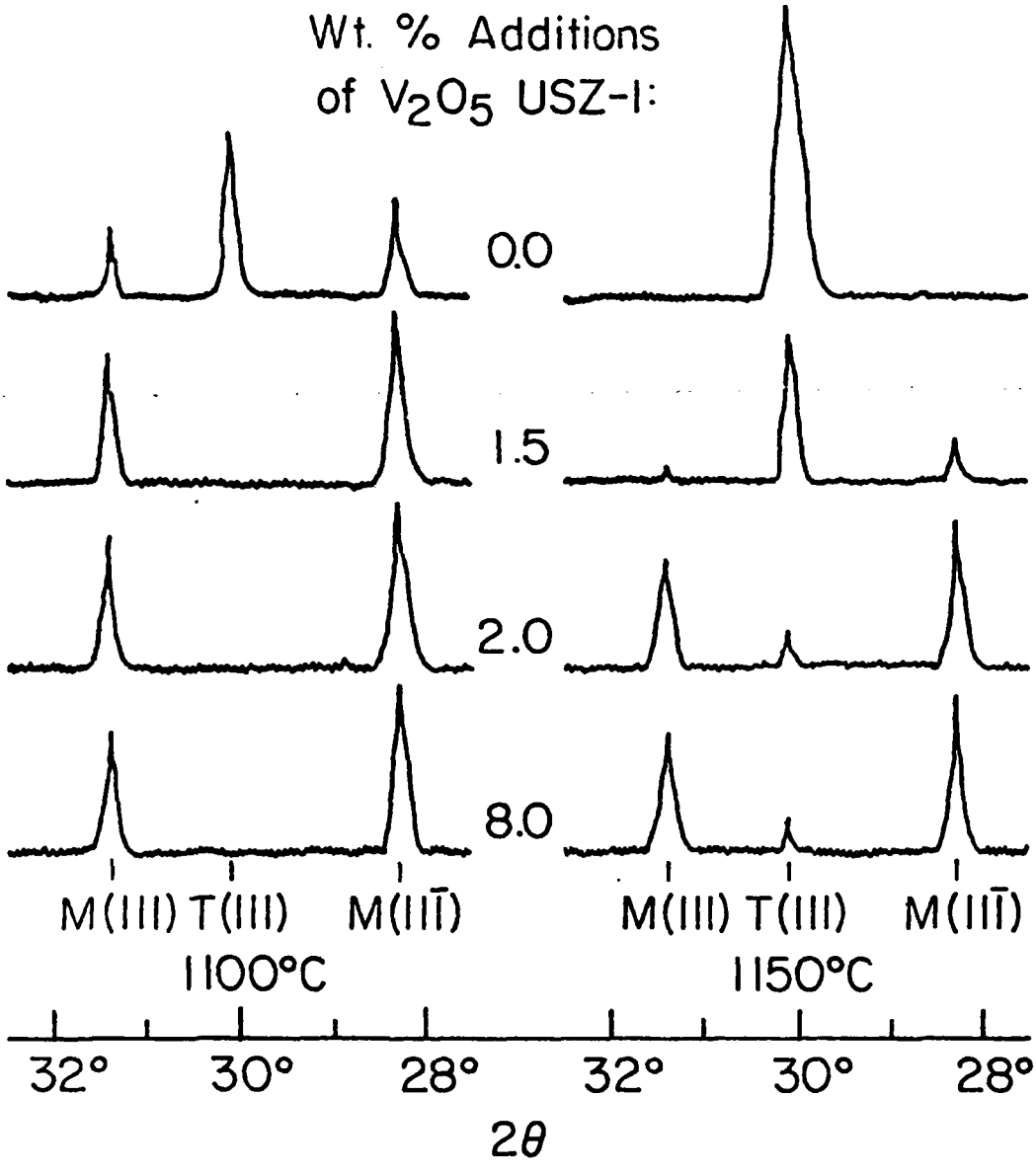

FIGURE 3. Hot stage X-ray diffraction data for ZrO_2 as a function of V_2O_5 content at 1100° and 1150°C.

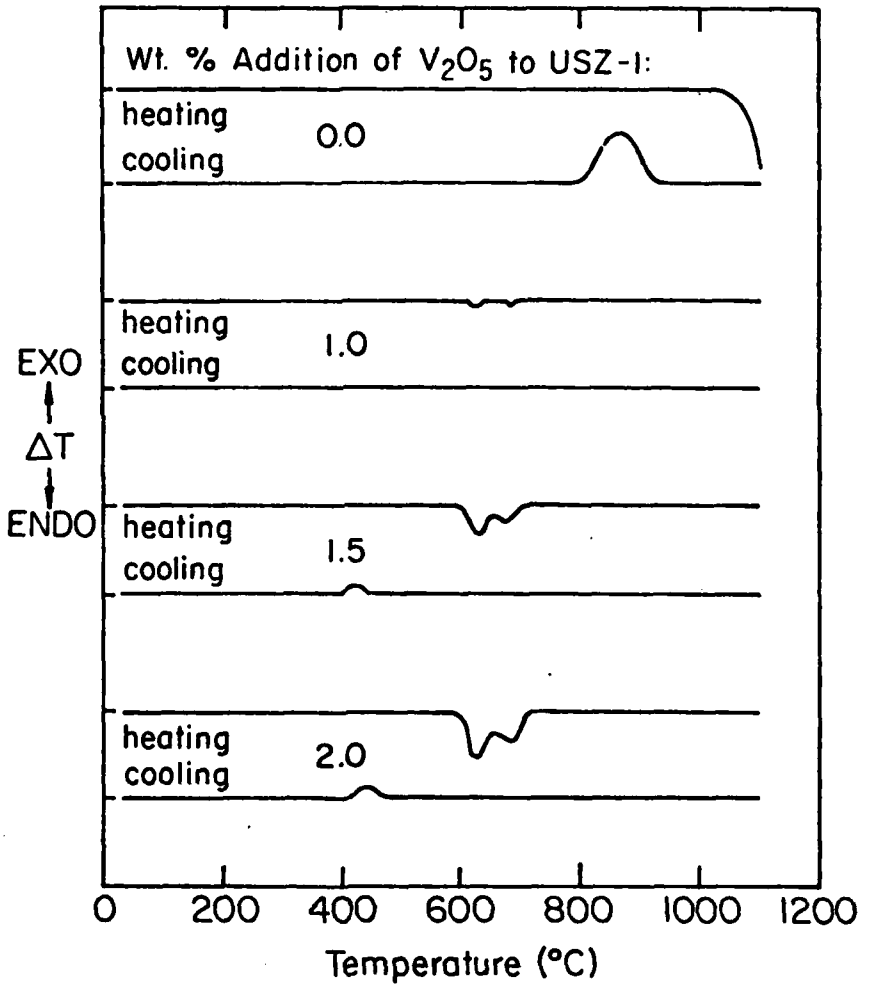

FIGURE 4. DTA heating and cooling curves for ZrO_2-V_2O_5 samples containing 0-2.0 wt% V_2O_5.

For samples containing $\geq$ 1 wt% V_2O_5, the transformation had not started by 1100°C. During heating of samples containing $\geq$ 1 wt% V_2O_5, two endotherms were observed between 600° and 700°C. These increased in size with V_2O_5 content. The second (smaller) endothermic peak occurred at ~ 685°C, corresponding closely to the melting point of V_2O_5 (~ 690°C). The first (larger) endothermic peak occurred at ~ 630° and apparently corresponded to the melting of a eutectic phase, although the binary eutectic for the ZrO_2-V_2O_5 system has been reported to be ~ 670°C .[15] Impurities in the starting powders could possibly have lowered the eutectic melting point. A single exotherm occurred at ~ 450°C during cooling of samples containing $\geq$ 1.5 wt% V_2O_5, and was attributed to crystallization of V_2O_5.

DTA heating curves of sintered ZrO_2 samples containing 0.0, 1.0, 1.5, and 2.0 wt% V_2O_5 are shown in Fig. 5 for the temperature range of 1000° to 1300°C. The data show an upward shift of the starting temperature for the monoclinic-tetragonal phase transformation, as the V_2O_5 content was increased. A reduction in the width of the transformation peak from ~ 160° for samples containing no V_2O_5 to ~ 35° for samples containing $\geq$ 2 wt% V_2O_5 was also observed. Besides the significant decrease in width, the transformation peak also became much larger in amplitude. However, the shape and position of the peak did not change for additions > 2 wt% V_2O_5.

Densification data for ZrO_2-V_2O_5 samples sintered at 1100°C for 24 h in air, are presented in Table 1. The data is given in terms of V_2O_5 content (1.5-15.0 wt%), percent theoretical density, forming pressure, green density and fired density. In general the fired densities for a given composition were observed to increase almost linearly with green density. This was true

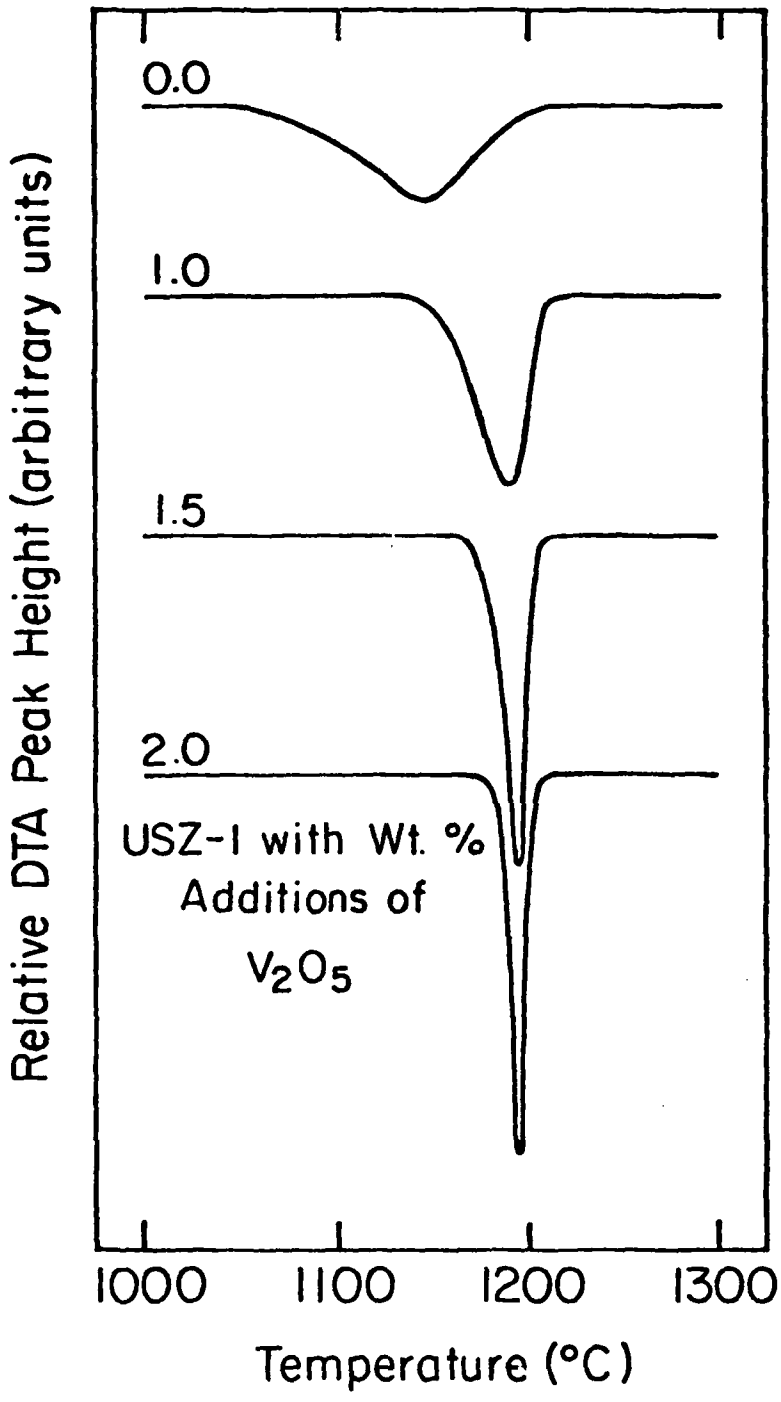

FIGURE 5. DTA heating curves for ZrO_2-V_2O_5 samples (0-2 wt% V_2O_5) showing a shift of the transformation temperature for the tetragonal phase with increasing V_2O_5 content.

TABLE 1
Densification Data for ZrO_2-V_2O_5 Samples
Sintered at 1100°C for 24 Hours

Wt% V_2O_5	Th. Density g/cm^3	Forming Pressure kpsi	Forming Pressure MPa	Green Density g/cm^3	Green Density % ThD	Fired Density g/cm^3	Fired Density % ThD
1.5	5.66	35	241	3.78	66.8	4.89	86.4
		50	345	3.87	68.4	5.06	89.4
2.0	5.62	35	241	3.78	67.3	5.00	89.0
		50	345	3.89	69.2	5.15	91.6
5.0	5.44	35	241	3.72	68.4	4.71	86.6
		50	345	3.83	70.4	4.71	86.6
8.0	5.27	35	241	3.79	71.9	4.80	91.1
		50	345	3.87	73.4	4.81	91.3
12.0	5.07	35	241	3.77	74.4	4.88	96.3
		50	345	3.85	75.9	4.89	96.4
15.0	4.94	35	241	3.59	72.7	4.85	98.2
		50	345	3.67	74.3	4.86	98.4

also for the relationship between green density and forming pressure, dictating the use of high forming pressures in most cases. The data shown are for forming pressures of 35 and 50 kpsi (241 to 345 MPa), where it may be noted that for V_2O_5 contents < 5.0 wt%, the higher forming pressure and density resulted in significantly higher fired densities. However, for V_2O_5 contents $\geq$ 5%, high green densities were evidently not as important due to the extensive particle rearrangement which took place during sintering.

The highest fired density (5.15 g/cm^3) was obtained for the 2 wt% V_2O_5 addition and the highest theoretical density (98.4% ThD) for the 15.0 wt% V_2O_5 addition. These latter samples were relatively fragile, however, owing to the low strength of the second phase and expansion mismatch between the solid phases. The theoretical density values were both measured pycnometrically and calculated from the expression given in Fig. 6 representing a series mixing relationship. Densities used were 5.76 g/cm^3 for ZrO_2 and 3.36 g/cm^3 for V_2O_5. As is evident from Fig. 6, the relationship between calculated and measured values was very close. Densification data as a function of time are given in Fig. 7 for ZrO_2 samples with 0.0, 1.5, 2.0 and 8.0 wt% V_2O_5. Comparison with the 0.0 V_2O_5 samples shows V_2O_5 to be an effective sintering aid for ZrO_2 at 1100°C. Densification generally increased with V_2O_5 content, but because of the low sintering temperature, limited solubility of ZrO_2 in the liquid phase, and moderately high dihedral angle (~ 40° at 1100°C), much longer sintering times ($\geq$ 8 hrs) were needed than would normally be required for the liquid phase (sintering) systems. The magnitude linear shrinkage for the ZrO_2-V_2O_5 samples were typically in the range of 6-8 percent for reasonable dense samples. This reflects the relatively high initial pressed densities.

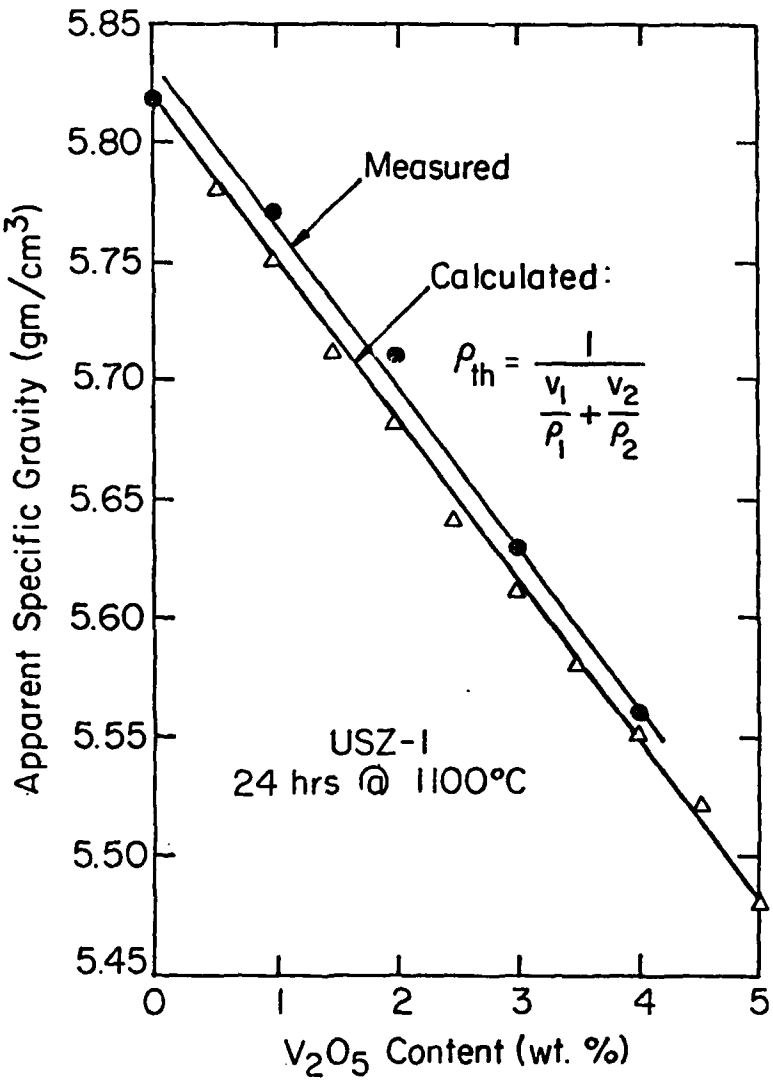

FIGURE 6. Comparison of measured and calculated theoretical density values for ZrO_2-V_2O_5 samples.

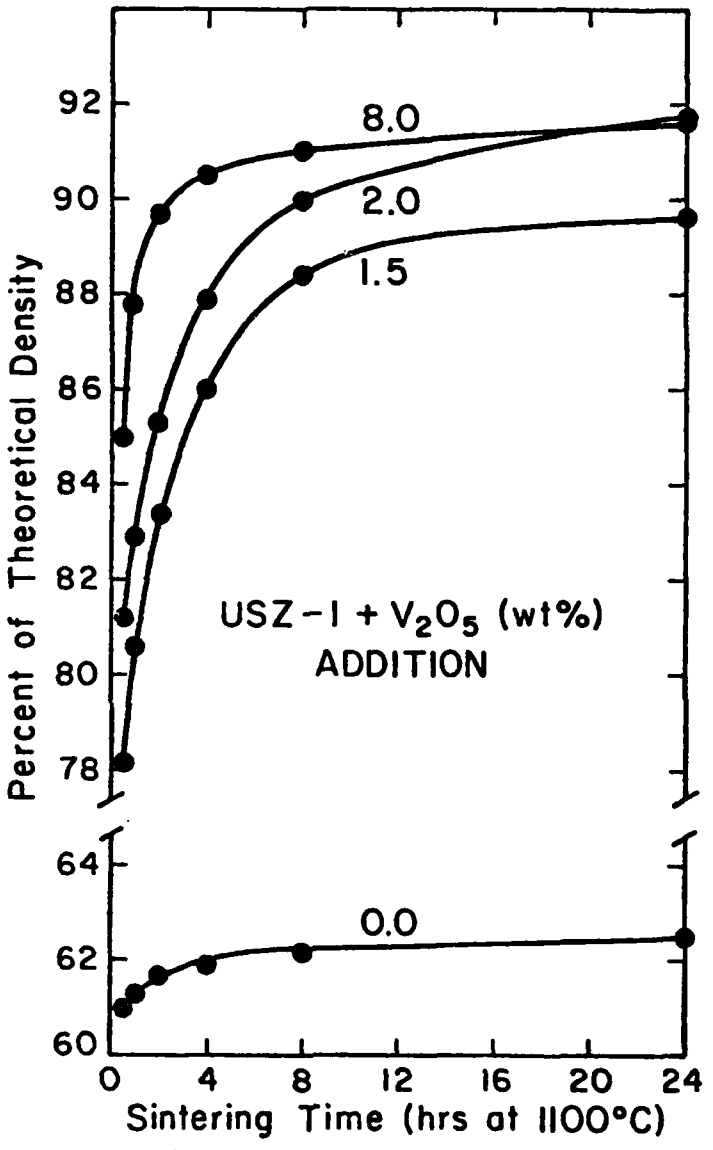

FIGURE 7. Percent of theoretical density vs. sintering time for ZrO_2 samples containing 1.5, 2.0, and 8.0 wt% V_2O_5.

Shrinkage data for some ZrO_2-V_2O_5 samples are given in Fig. 8. These curves, as would be expected, show the same kinetic behavior as the densification. Figure 9 shows a plot of percent theoretical density as a function of V_2O_5 content for samples formed at a pressure of 35 kpsi (241 MPa) and sintered at 1100°C for soak times up to 24 h. Two regions of relatively high densification were observed to occur as a function of V_2O_5 content, especially noticeable for soak times in excess of 30 min. Density maxima occurred at ~ 2 wt% and 12 wt% V_2O_5, giving a distinctly bimodal appearance to the densification curves. As the V_2O_5 content was increased above 2 wt%, the density decreased until a minimum was reached at ~ 6 wt%, above which the density increased again. This behavior was similar to that observed by Dereberya and Kogut[22] as shown in Fig. 10, although in their study of the ZrO_2-V_2O_5 system the fired densities obtained were somewhat lower and the maxima also occurred at lower V_2O_5 additions.

An explanation for the observed biomodal densification behavior can be given with reference to Fig. 11, which shows the relative density versus V_2O_5 content curve with regions I, II, and III representing different densification mechanisms.

The degree of densification obtained from rearrangement of spherical particles has recently been regarded as a direct function of the force existing between particles connected by a liquid bridge.[23,24] Calculations of the interparticle force indicate that the attractive forces are highest at low liquid contents and decrease as the liquid content increases. Experimental evidence supporting the results of these calculations was supplied by Huppmann and Riegger.[24] They found that the most pronounced rearrangement in arrays of spherical tungsten particles during sintering was obtained from particle rearrangement.

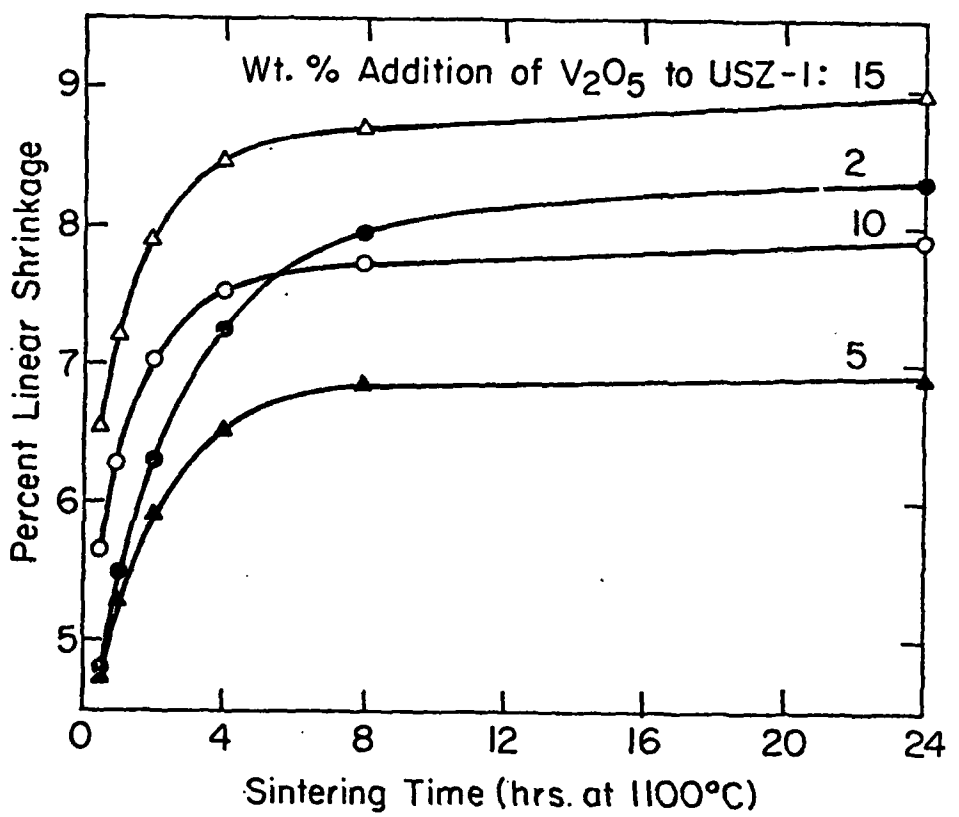

FIGURE 8. Percent linear shrinkage versus sintering time for ZrO_2-V_2O_5 samples.

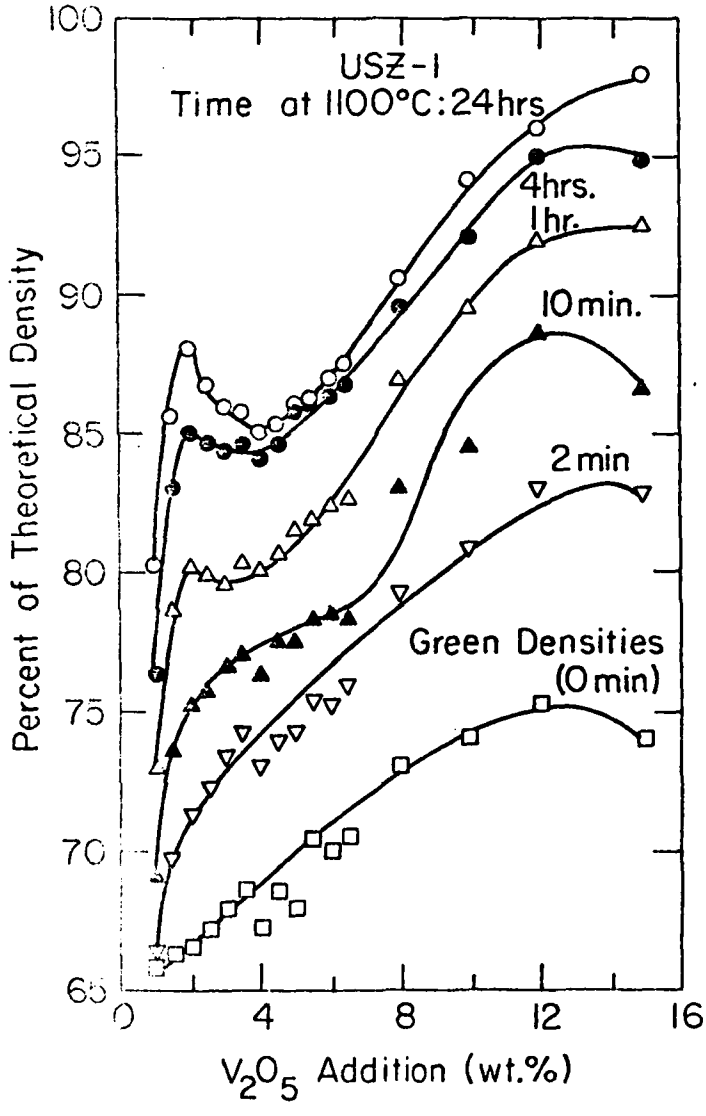

FIGURE 9. Percent theoretical density versus wt% V_2O_5 and soak times for ZrO_2-V_2O_5 samples sintered at 1100°C.

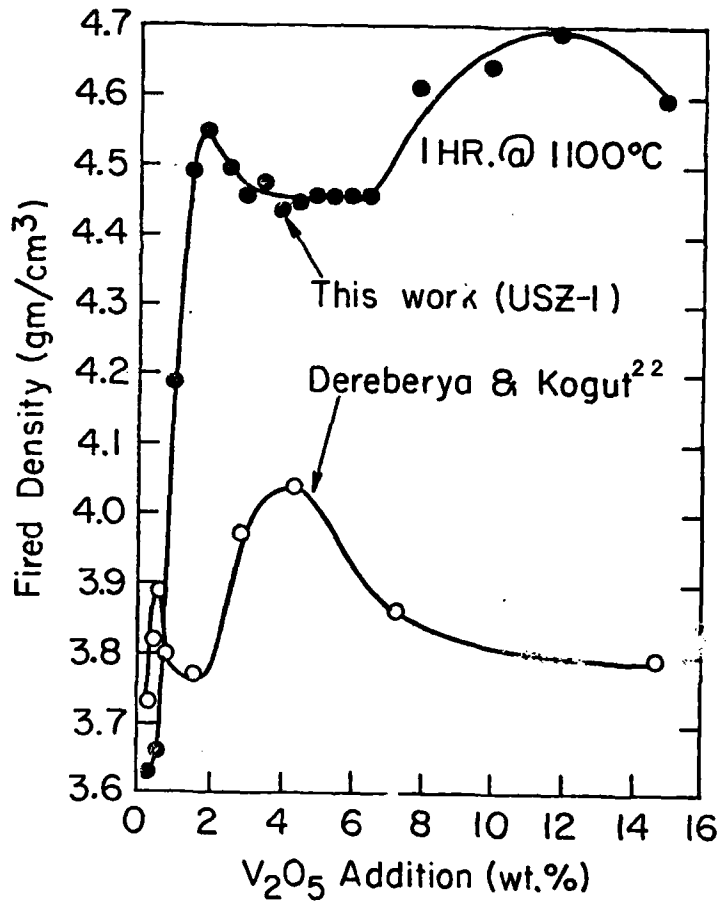

FIGURE 10. Comparison of fired density data showing density maxima as a function of V_2O_5.

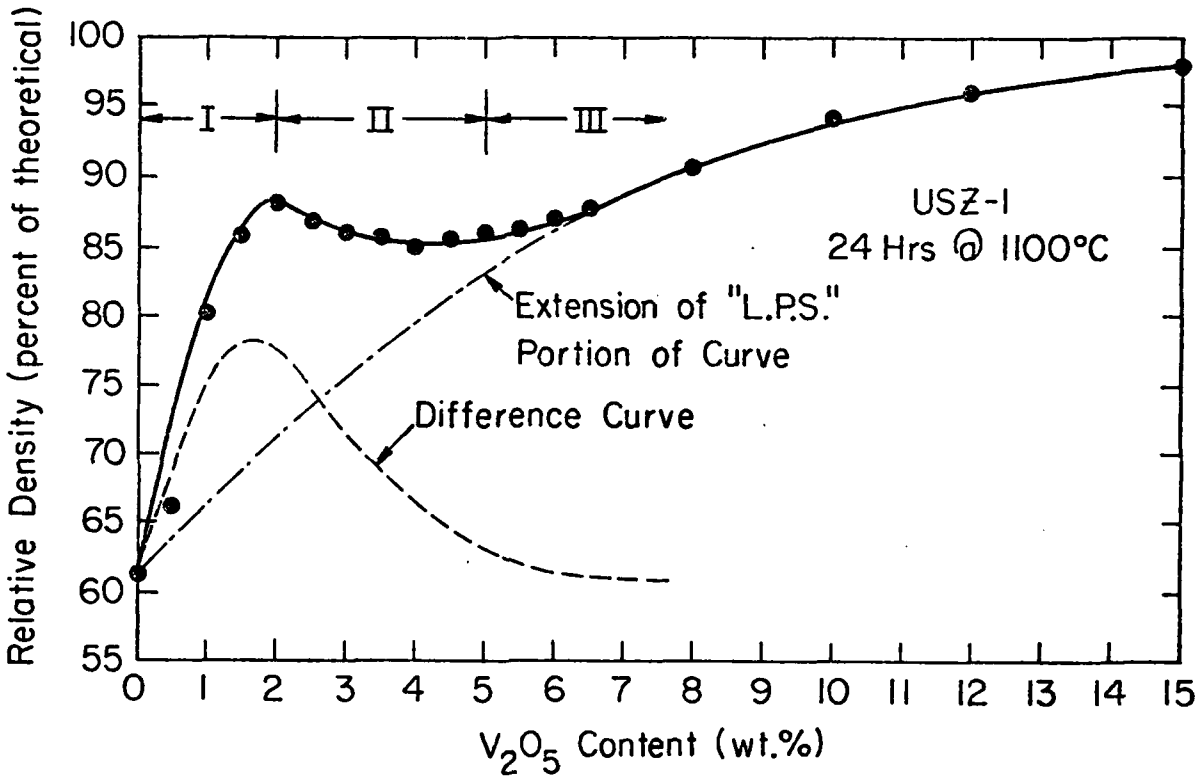

FIGURE 11. Relative density curve illustrating regions (I, II, III) of different densification mechanism as a function of V_2O_5 content at 1100°C/24 h.

From this analysis, the densification for region I in Fig. 11, is attributable mainly to particle rearrangement due to the low liquid content (~ 5 vol% liquid for 2 wt% V_2O_5) and resultant high hydrostatic forces. Region III, in contrast, would densify mainly by solution-precipitation processes since with > 15 vol% liquid (> 6 wt% V_2O_5) the interparticle attractive forces would be relatively weak. Both regions I and III should show monotonic increases in density over the composition ranges to which they apply. In region II, both densification mechanisms evidently apply, except that with too little liquid for efficient solution-precipitation and too much for efficient particle rearrangement, particle bridging and solid-solid contact (resistive) conditions would predominate. This in turn would lead to a decrease in density. The density maximum (Fig. 11) at the 2 wt% V_2O_5 addition, therefore, represent an optimum balance between the attractive forces (due to capillary action) and the resistive forces (due to frictional contact between particles).

B. Microstructural Analysis

SEM photomicrographs of the fracture surfaces of sintered ZrO_2 samples containing 1.0, 1.5, 2.0, and 8.0 wt% V_2O_5 are shown in Fig. 12. Intergranular fracture is clearly indicated by the presence of second phase areas on the surfaces of the ZrO_2 grains. The second phase was not as evident for the 1.0 wt% V_2O_5 samples, and as expected, the quantity of second phase observed increased with V_2O_5 content. In addition, the grain size increased substantially with V_2O_5 content.

SEM photomicrographs of polished, thermally etched surfaces of sintered samples containing 1.5, 2.0, 4.0, and 8.0 wt% V_2O_5 are shown in Fig. 13. The ZrO_2 grains show a flattened polyhedral shape typical of many liquid phase sintering systems for which the content of liquid phase is relatively

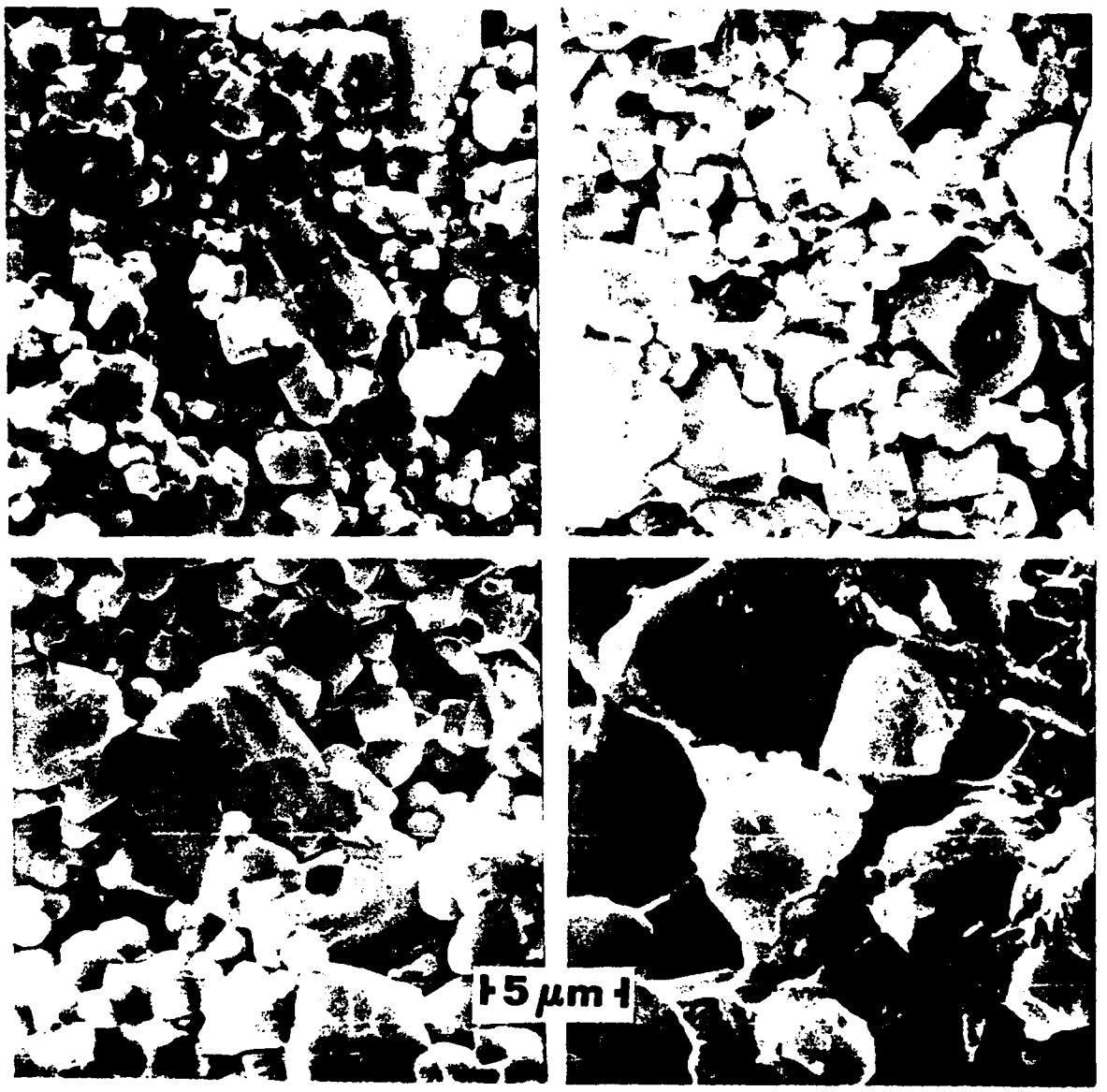

FIGURE 12. SEM photomicrographs of fracture surfaces of ZrO_2 samples containing: a) 1.0, b) 1.5, c) 2.0, and d) 8.0 wt% V_2O_5.

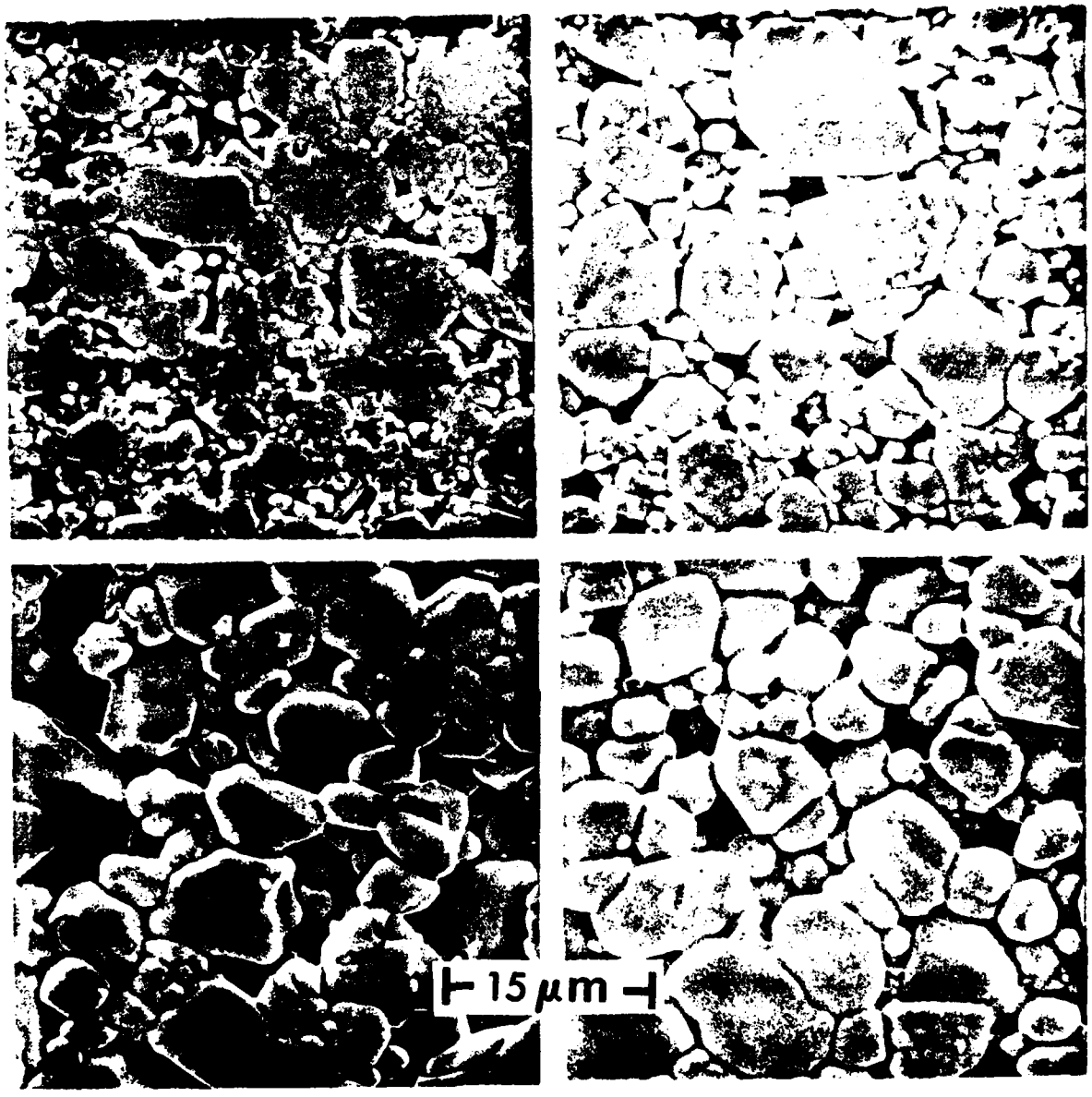

FIGURE 13. SEM photomicrographs of polished, thermally etched surfaces of ZrO_2 samples containing: a) 1.5, b) 2.0, c) 4.0, and d) 8.0 wt% V_2O_5.

low. The large ZrO_2 grains in the 1.5 wt% sample (Fig. 13a) appear to be composite grains formed from particles comparable in size to those of the milled, unfired powder (~ 1.0 μm). This subgrain structure indicated that grain growth in samples containing small amounts of V_2O_5 occurred mainly by a particle agglomeration mechanism.[25] As the V_2O_5 content of the samples increased from 1.5 to 8.0 wt%, the average size of the grains increased. However, this increase in average size was due mainly to a decrease in the number of smaller grains, indicating that larger grains grew at the expense of smaller grains (Ostwald ripening). Grain growth, therefore, most likely occurred by a combination of particle agglomeration (dominant at low liquid contents) and Ostwald ripening (dominant at high liquid contents).

The average fired grain size is shown plotted as a function of V_2O_5 content in Fig. 14. Essentially no grain growth occurred until the V_2O_5 content exceeded 1 wt%. Above 4 wt% V_2O_5, the grain growth was relatively insensitive to the quantity of liquid present. Since grain growth for high V_2O_5 contents had been attributed mainly to solution-precipitation, it follows that the rate-controlling step in this process was solution of ZrO_2 at the solid-liquid interface.

Figure 15a is a TEM photomicrograph of a ZrO_2-2 wt% V_2O_5 sample showing a multiple-grain intersection containing a second phase (region A) which extends into an adjacent grain boundary (region B). This boundary region is shown at a higher magnification in Fig. 15b. A microdiffraction pattern of region A and EDAX spectra of regions A, B, and C (taken from the ZrO_2 grain at a distance of ~ 400 Å from the edge of the intergranular phase) are shown in Figs. 15c, d, e, and f, respectively. The microdiffraction pattern indicated that the second phase was amorphous. The EDAX spectrum from region A (Fig. 15d) shows that the second phase contained mainly vanadium,

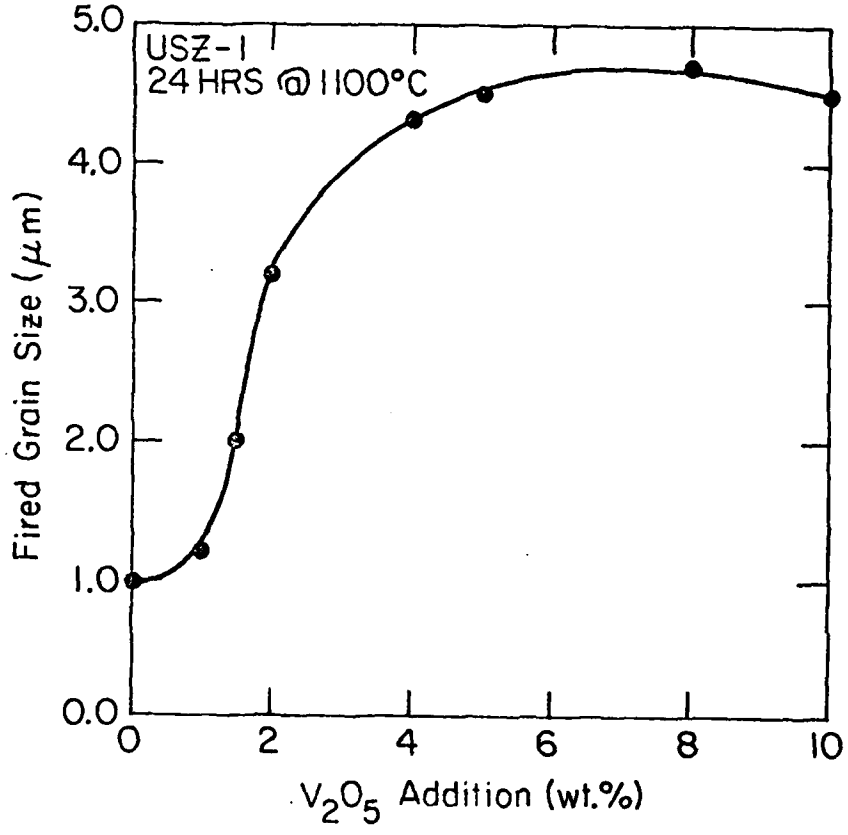

FIGURE 14. Fired grain size vs V_2O_5 content of ZrO_2 samples.

FIGURE 15. ZrO_2 sample containing 2 wt% V_2O_5: a) TEM photomicrograph showing multiple-grain junction containing second phase (region A) which extends into an adjacent grain boundary (region B), b) higher magnification of boundary region (region B), c) microdiffraction pattern of second phase (region A), and EDAX spectra of: d) region A, e) region B, and f) region C (taken from ZrO_2 grain ~ 400 Å from edge of second phase).

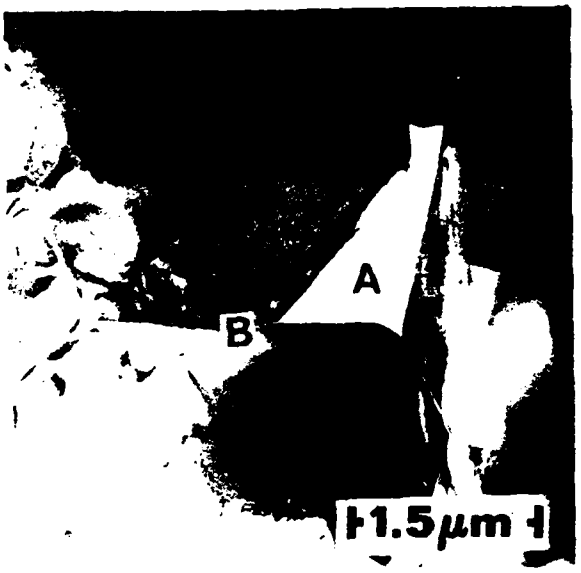
A
B
1.5μm

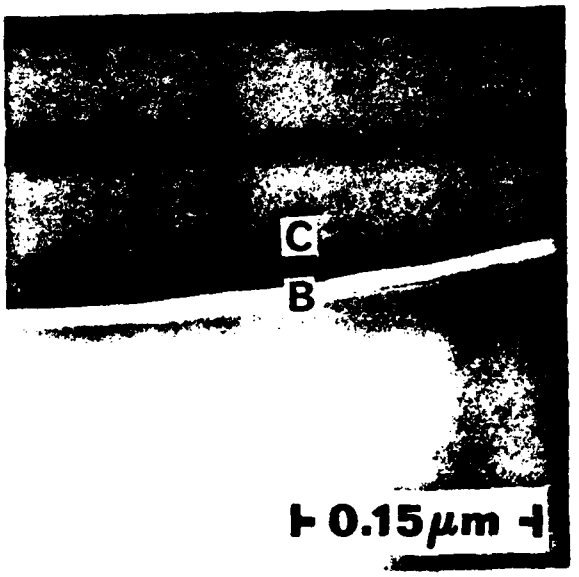
C
B
0.15μm

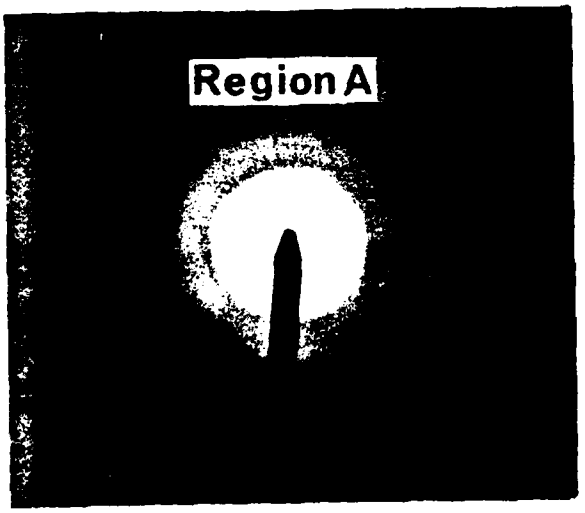
Region A

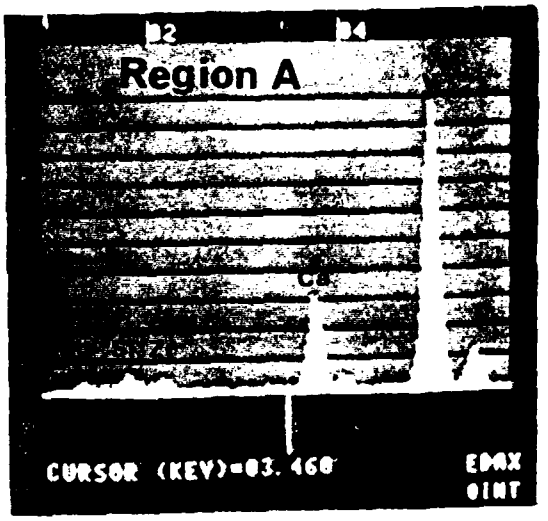
Region A
Ca
CURSOR (KEV)=03.460
EDAX
0INT

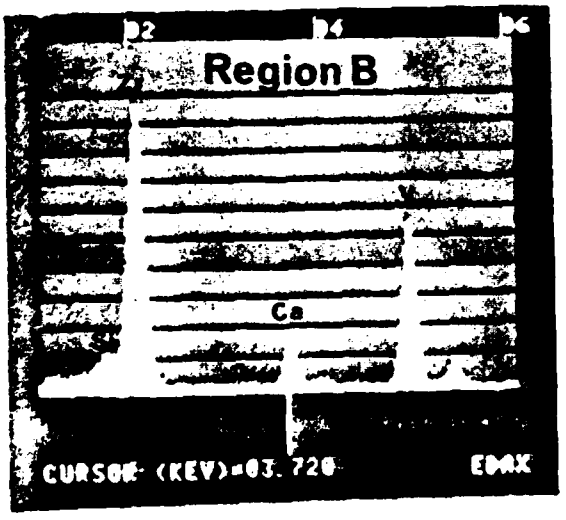
Region B
Ca
CURSOR (KEV)=03.720
EDAX

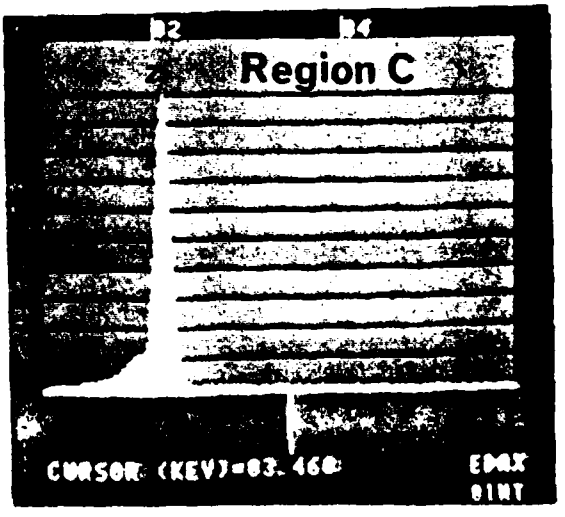
Region C
CURSOR (KEV)=03.460
EDAX
0INT

with a substantial amount of calcium and minor amounts of zirconium, silicon, and magnesium. The presence of zirconium was expected, due to the limited solubility of ZrO_2 in the liquid phase. The calcium, silicon, and magnesium originated as oxide impurities in the ZrO_2 powder which segregated to the intergranular regions. The EDAX spectrum from the grain boundary (Fig. 15e) shows the presence of the second phase. However, since the boundary phase was only ~ 150 Å wide, a large portion of the characteristic X-rays originated in the surrounding ZrO_2 grains due to beam spreading. The sharpness of the composition gradient in the grain boundary region is shown by the EDAX spectrum (Fig. 15f) collected ~ 400 Å away from the edge of the intergranular phase (region C). With the possible exception of silicon, no impurities were detected within the ZrO_2 grains.

Approximate elemental compositions, determined from the EDAX data for the second phase, are listed in Table 2 for ZrO_2 samples containing 1.5 and 2.0 wt% V_2O_5. The equivalent oxide compositions, also given in Table 2, would be expected to form glassy second phases, which would account for the amorphous microdiffraction pattern observed.

DTA and hot-stage X-ray analysis showed that additions of V_2O_5 up to 2 wt% increased the starting temperature of the monoclinic-tetragonal phase transformation from ~ 1050°C for 0 wt% to ~ 1150°C for 2 wt%. For V_2O_5 additions > 2 wt%, the starting temperature remained constant at ~ 1150°C, indicating that a solubility limit of vanadium ions in the ZrO_2 lattice had been reached. However, it was determined from emission spectrographic analysis of a ZrO_2-2 wt% V_2O_5 sample (repeatedly milled and washed to remove the intergranular phase) that the vanadium content (Table 2) within the ZrO_2 grains was $\leq$ 0.2 at.% (~ 0.15 wt% V_2O_5 or V_2O_4). The low vanadium content in the ZrO_2 grains was consistent with the data obtained from the XRD

TABLE 2: Composition of Intergranular Phase

(From EDAX Data)

	1.5 wt% V_2O_5		2.0 wt% V_2O_5	
Element	At.%	Equivalent Wt% Oxide	At.%	Equivalent Wt% Oxide
$V_{K\alpha}$	65.7	V_2O_5: 74.8	74.4	V_2O_5: 81.4
$Ca_{K\alpha}$	26.8	CaO : 18.7	19.6	CaO : 13.2
$Zr_{K\alpha}$	2.1	ZrO_2: 3.2	2.1	ZrO_2: 3.0
$Si_{K\alpha}$	2.9	SiO_2: 2.2	2.4	SiO_2: 1.7
$Mg_{K\alpha}$	2.5	MgO : 1.3	1.5	MgO : 0.7

Vanadium Content of ZrO_2 Grains:

(From Emission Spectrographic Analysis)

Vanadium Content $\lesssim$ 0.2 At.%.

analysis, which showed no changes in the monoclinic lattice parameters as a function of V_2O_5 content. With no change in the lattice parameters and only a small percentage of the vanadium in the V^{4+} state (qualitatively determined from EPR studies, Fig. 16), and taking into account charge and size considerations, it was concluded that V^{4+}, rather than V^{5+}, ions diffused into the ZrO_2 lattice.

The percent weight loss of ZrO_2-V_2O_5 samples is shown in Fig. 17 as a function of V_2O_5 content. The uniformly low loss for V_2O_5 contents $\leq$ 1.5 wt% indicated that the V_2O_5 was effectively tied up in the glassy second phase. However, as the V_2O_5 content was increased above 1.5 wt%, the effects of the impurities were diluted and the properties of the second phase approached more nearly those of pure V_2O_5 (which has a relatively high vapor pressure at 1100°C[25]).

C. Fired Properties

The dc electrical conductivity data for ZrO_2 samples containing 1.5 and 2.0 wt% V_2O_5 are shown plotted in Fig. 18 as a function of the inverse absolute temperature. The conductivity of the 1.5 wt% sample was the same for heating and cooling; however, for the 2 wt% sample, the conductivity abruptly increased at ~ 450°C during cooling. This behavior can be attributed to partial crystallization of V_2O_5 from the intergranular phase, indicated by a DTA exotherm observed at ~ 450°C and the increased conduction which would result from the crystallization of V_2O_5.[3] Crystallization of V_2O_5 was, however, not confirmed by microdiffraction, possibly because the crystallites were extremely small. In contrast, the linear conduction behavior for samples with $\leq$ 1.5 wt% V_2O_5 would indicate the absence of crystalline V_2O_5, the added V_2O_5 being tied up in the glassy intergranular phase.

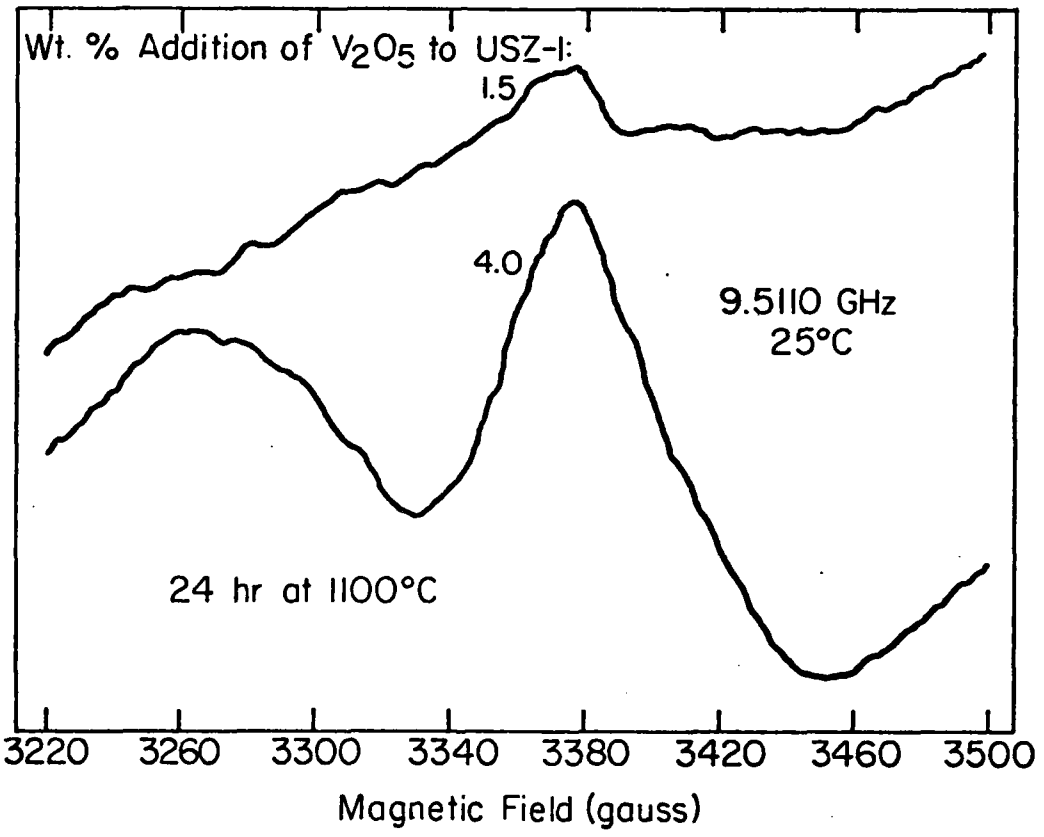

FIGURE 16. EPR data showing V^{4+} paramagnetic peaks in fired ZrO_2 samples with 1.5 wt% and 4.0 wt% V_2O_5.

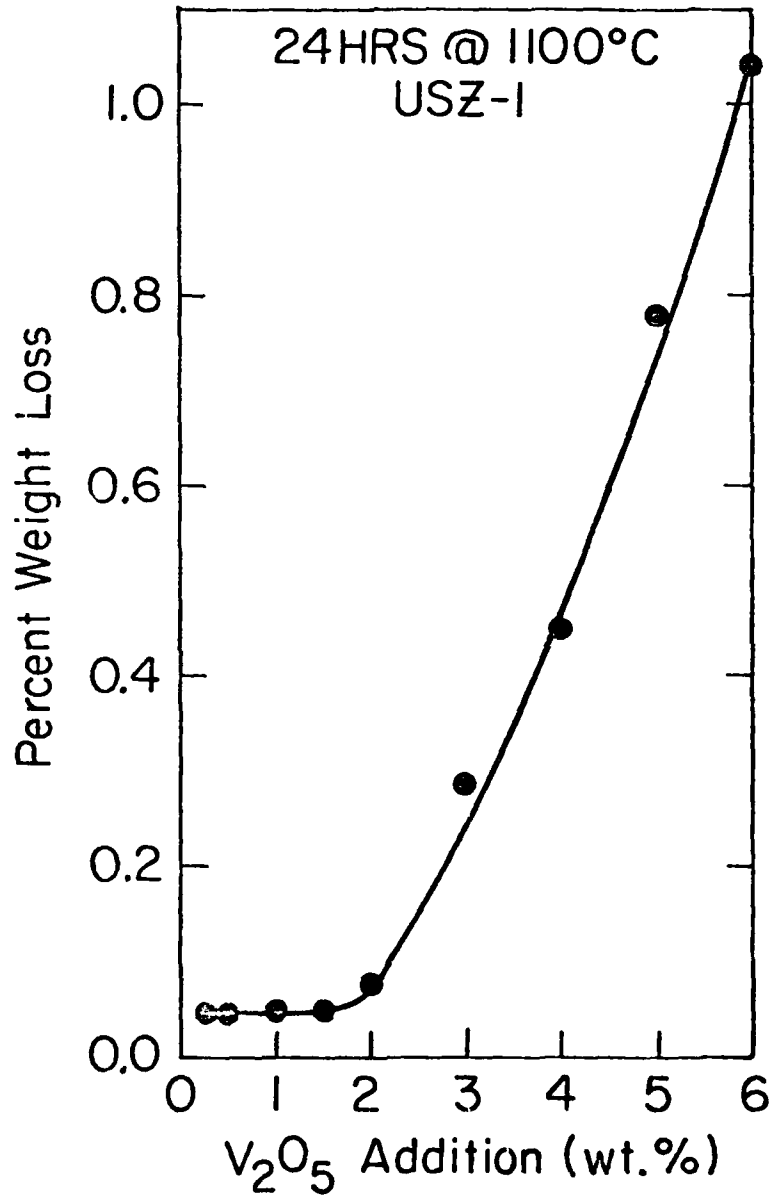

FIGURE 17. Percent weight loss as a function of V_2O_5 content of ZrO_2 samples.

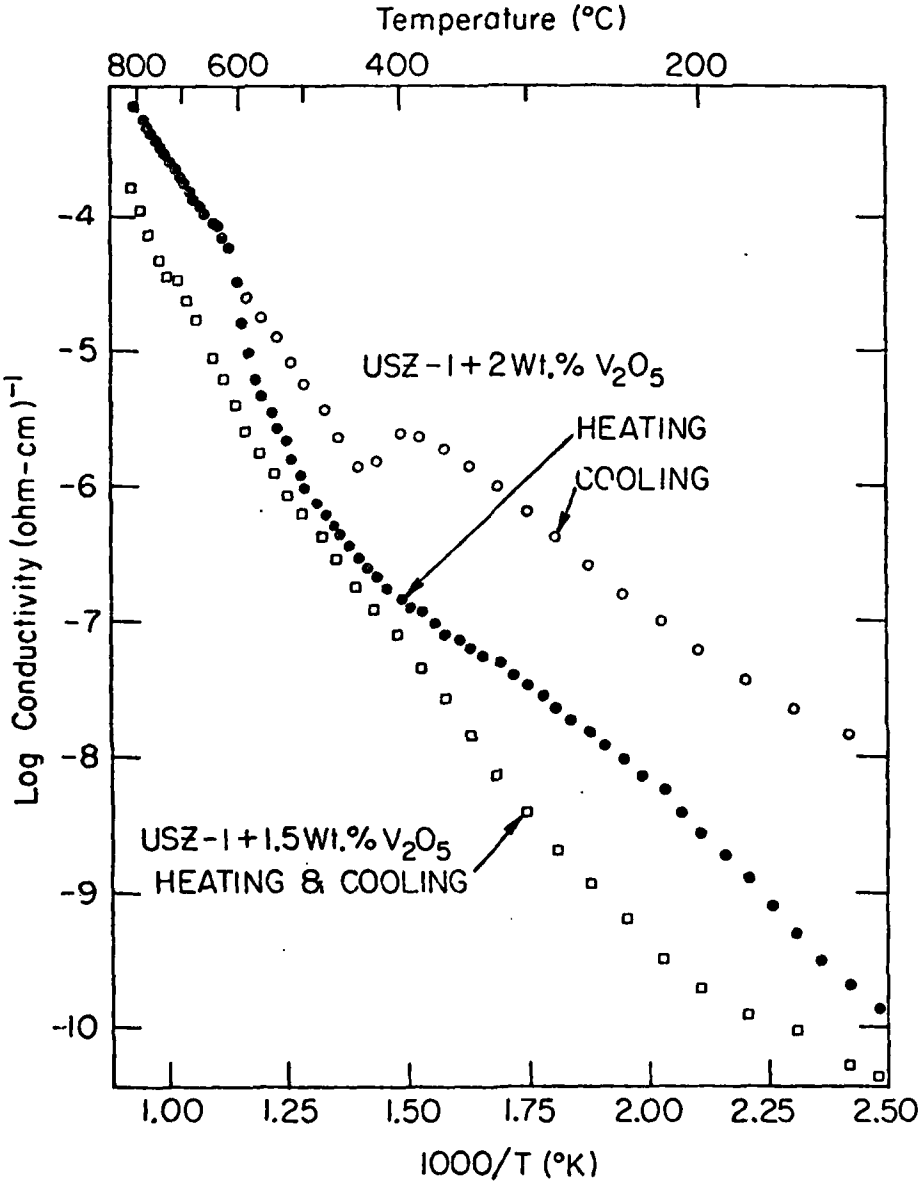

FIGURE 18. Log conductivity vs inverse absolute temperature for ZrO_2 samples containing 1.5 and 2.0 wt% V_2O_5.

The thermal expansion (up to 950°C) of a ZrO_2-1.5 wt% V_2O_5 sample is shown in Fig. 19. The expansion was linear with the relatively low expansion coefficient of $5.6 \times 10^{-6}/°C$, which is consistent with the existence of a glassy intergranular phase of relatively low expansion. For greater V_2O_5 contents, the expansion became nonlinear due to the large (~ 30 vol%) expansion of V_2O_5 upon melting.[3]

Table 3 summarizes the fired properties for ZrO_2 samples containing 1.5, 2.0, and 8.0 wt% V_2O_5. The 1.5 wt% samples exhibited the best overall fired properties. The 1.5 wt% addition evidently produced a sufficient quantity of liquid (~ 4.0 vol%) to cause a high degree of densification. The presence of impurities resulted in the formation of a glassy second phase. This aided sintering and essentially determined the characteristics of the fired properties. As the V_2O_5 content was increased above 1.5 wt%, the properties became increasingly dominated by the intergranular phase. In general, larger quantities of V_2O_5 increased the thermal expansion and electrical conductivity and decreased the strength of the samples, as would be expected.

IV. Conclusions

1. Addition of V_2O_5 (1.5-2.0 wt%) to monoclinic ZrO_2 powders (avg ps ~ 1 μm) resulted in dense ceramic compacts (90-92% ThD) when sintered in air at 1100°C for 24 h.
2. Densification and grain growth were determined by rearrangement and solution-precipitation processes for which the rate-controlling step was found to be solution of ZrO_2 at the solid-liquid

Table 3. Summary of Fired Properties for ZrO_2-V_2O_5 Samples

Wt% V_2O_5	Average Fired Density g/cm^3	%ThD	Expansion Coeff. $10^{-6}/°C$	Elec. Cond. 800°C $10^{-4}(ohm\text{-}cm)^{-1}$	Calc. Flex. Strength kpsi	MPa
1.5	5.06	89.5	5.6	2.0	22	152
2.0	5.15	91.6	6.0	6.5	23	159
8.0	4.81	91.3	6.9	120.0	18	124

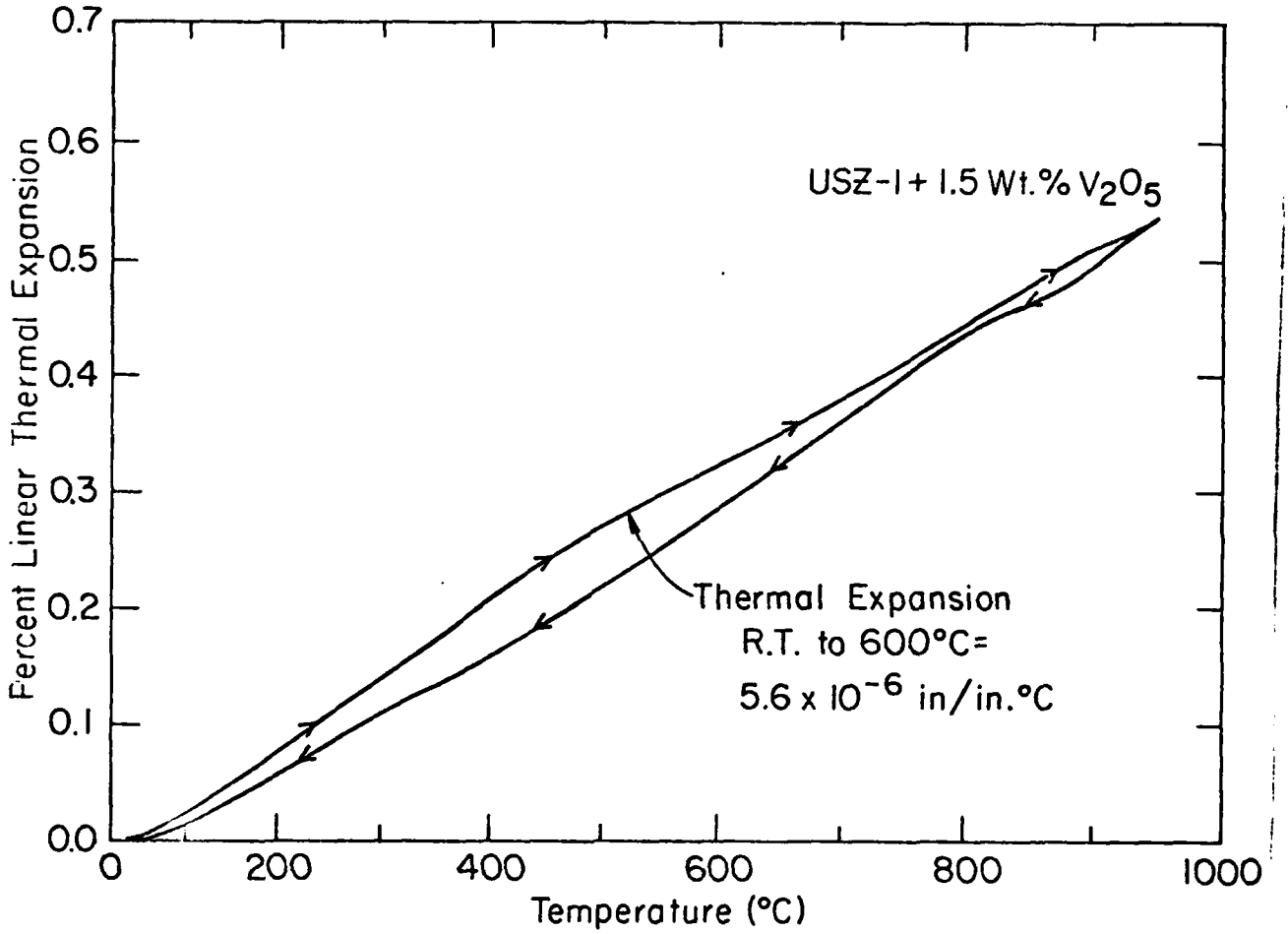

FIGURE 19. Thermal expansion to 950°C of ZrO_2 sample containing 1.5 wt% V_2O_5.

interface. Solubility of vanadium (as V^{4+}) in the ZrO_2 phase was low.

3. For V_2O_5 contents < 2 wt%, an amorphous intergranular phase, observed from the microstructures, essentially determined the properties of the fired compacts. For V_2O_5 contents > 2 wt%, crystallization of V_2O_5 from the intergranular phase tended to degrade the properties.

4. Properties measured for sintered compacts (1.5 wt%) were: $\alpha = 5.6 \times 10^{-6}/°C$; $\sigma(800°C) = 2.0 \times 10^{-4}$ $(ohm\text{-}cm)^{-1}$; and $S_R = 152$ MPa, comparable to those of bulk ZrO_2.

V. Acknowledgements

This work was supported by the Office of Naval Research under Contract No. N-00014-78-0279 and in part by the National Science Foundation under the MRL grant DMR-80-20250.

VI. References

1. R. C. Garvie, ''Zirconium Dioxide and Some of its Binary Systems,'' High Temperature Oxides, Vol. 5, Part II, ed. by A. M. Alper, Academic Press, New York (1970), pp. 117-163.

2. E. Ryshkewitch, Oxide Ceramics, Academic Press, New York (1960) pp. 350-396.

3. T. Allersma, R. Hakim, T. N. Kennedy, and J. D. Mackenzie, ''Structure and Physical Properties of Solid and Liquid Vanadium Pentoxide,'' Tech. Report No. 2, Contract No. NONR-591(21), Rensselear Polytechnic Institute (1966).

4. A. Burdese and M. L. Borlera, ''The System of ZrO_2-V_2O_5,'' Ann. Chim. (Rome), 50, 1570-72 (1960).

5. B. S. Cherepanov, ''Peculiarities in the Formation of Zirconium-Vanadium Colors,'' Glass and Ceramics, 22, 367-69 (1965).

6. G. K. Layden and M. C. McQuarrie, ''Effect of Minor Additions on Sintering of MgO,'' J. Am. Ceram. Soc., 42[2], 89-92 (1959).

7. D. Alvarez-Estrada and P. D. Botia, ''Effect of Vanadium Pentoxide on the Sintering and Grain Growth of Magnesium Oxide,'' Bol. Soc. Esp. Ceram., 5[2] 201-13 (1966).

8. L. C. F. Blackman, ''On the Defect Structure and Sinterability of Magnesium Ferrite,'' Trans. Brit. Ceram. Soc., 63[7] 331-45 (1964).

9. J. Kulikowski, ''Sintering of Ni-Zn Ferrites in the Presence of V_2O_5,'' Sov. Powd. Met. Metal Ceram., 12[7] 597-99 (1973).

10. A. P. Mozhaev, N. N. Oleinikov, N. S. Shumilkin, and V. I. Fadeeva, ''Reaction of Lithium Ferrite with Small Amounts of Low-Melting Additives,'' Inorganic Materials, 13[5] 718-20 (1977).

11. D. E. Wittmer and R. C. Buchanan, ''Low-Temperature Densification of Lead Zirconate Titanate with Vanadium Pentoxide Additive,'' J. Am. Ceram. Soc., 64[8] 485-90 (1981).

12. G. Peyronel, ''Vanadates of Zirconium: I,'' Gazz. CHIM. Ital., 72 77-83 (1942).

13. B. W. King and L. L. Suber, ''Some Properties of the Oxides of Vanadium and their Compounds,'' J. Am. Ceram. Soc., 38[9] 306-11 (1955).

14. V. Cirilli, A. Burdese, and C. Brisi, ''La Corrosione Di Legne Refrattario Da Parte Di Ceneri Di Petrolio Contenti Vanadio,'' Atti Della Accademia Delle Science Di Torino, 95[1] 209-10 (1960-61).

15. D. Craig and F. A. Hummel, ''Zirconium Pyrovanadate Transitions,'' J. Am. Ceram. Soc., 55[10] 532 (1972).

16. A. S. Bystrikov and B. S. Cherepanov, ''X-ray Investigation of Tone Formation of Zircon in the SiO_2-V_2O_6-ZrO_2 System,'' Russ. J. Inorganic Chem., 9[5] 654-56 (1964).

17. T. Demiray, D. K. Nath, and F. A. Hummel, ''Zircon-Vanadium Blue Pigment,'' J. Am. Ceram. Soc., 53[1] 1-4 (1970).

18. V. I. Matkovich and P. M. Corbett, ''Formation of Zircon from Zirconium Dioxide and Silicon Dioxide in the Presence of Vanadium Pentoxide,'' J. Am. Ceram. Soc., 44[3] 128-30 (1961).

19. A. S. Bystrikov, ''The Mechanism of the Formation of Zirconium-Silicon-Vanadium and some other Ceramic Pigments,'' Glass and Ceramics, 22 367-69 (1965).

20. I. A. Dmitriev, ''Role of V_2O_5 in the Synthesis of Beryllium Orthosilicate,'' J. Inorganic Materials (USSR), 13[3] 564-65 (1977), ibid. 92[6] 1009-11 (1973) (English Transl.).

21. S. Tacvorian, ''Acceleration of Sintering in a Single Phase; Consideration of the Mechanism for Minor Additions,'' Compt. Rendu, 234 2363-65 (1952).

22. N. A. Dereberya and V. M. Kogut, ''Some Physical Properties of ZrO_2 with Admixture of V_2O_5,'' Fiz. Elek. Resp. Mezhved. Nauch., 46-50 (1975).

23. W. J. Huppmann, ''Sintering in the Presence of Liquid Phase,'' Sintering and Catalysis, Ed. by G. C. Kuczynski, Plenum Press, NY and London, pp. 359-78 (1975).

24. W. J. Huppmann and H. Riegger, ''Modelling of Rearrangement Processes in Liquid Phase Sintering,'' Acta Met., 23[8] 965-71 (1975).

25. T. J. Whalen and M. Humenik, ''Mechanisms and Microstructural Aspects of Liquid Phase Sintering,'' Prog. in Powder Met., 18 85-98 (1962).

VII. Summary of Work Accomplished Under Contract No. US Navy-N-00014-78-C-0279

1. Reports

Reports issued under this contract include the following:

a. D. E. Wittmer and R. C. Buchanan, ''Densification of PZT Ceramics with V_2O_5 Additive,'' (ONR Report # 1), University of Illinois, Urbana, IL (Jan. 1979).

b. H. D. DeFord and R. C. Buchanan, ''Low Temperature Densification of ZrO_2 with Vanadate Additive,'' (ONR Report # 2), University of Illinois, Urbana, IL (July 1979).

c. A. Sircar and R. C. Buchanan, ''Densification of Zirconia with Borates,'' (ONR Report # 3), University of Illinois, Urbana, IL (Jan. 1980).

d. R. C. Buchanan and H. D. DeFord, ''Densification of Monoclinic ZrO_2 with Vanadate Additives,'' (ONR Report # 4), University of Illinois, Department of Ceramic Engineering, Urbana, IL (July, 1982).

2. Thesis

a. D. E. Wittmer, ''Low Temperature Densification of Lead Zirconate Titanate with Vanadium Pentoxide Additions,'' Ph.D. Thesis, University of Illinois, Urbana, 1980.

b. G. Wolter, ''Properties of Hot Pressed ZrV_2O_7,'' M.S. Thesis, University of Illinois, Urbana, 1981.

c. H. D. DeFord, ''Low Temperature Densification of Zirconium Dioxide with Vanadate Additives,'' M.S. Thesis, University of Illinois, Urbana, 1982.

3. Papers

a. D. E. Wittmer and R. C. Buchanan, ''Low Temperature Densification of Lead Zirconate Titanate with Vanadium Pentoxide Additive,'' J. Am. Ceram. Soc., 64[8] 485-90 (1981).

b. A. F. Grandin de l'Eprevier and R. C. Buchanan, ''Preparation and Properties of $Ca_2V_2O_7$ Single Crystals,'' J. Electrochem. Soc., (1982).

c. R. C. Buchanan, H. D. DeFord, and R. W. Doser, ''Effects of Vanadate Phase on Sintering and Properties of Monoclinic ZrO_2,'' Advances in Ceramics, Vol. II, [Grain Boundary Phenomena in Electronic Ceramics] American Ceramic Society (1982).

d. A. Sircar and R. C. Buchanan, ''Densification and Phase Changes in CaO-stabilized ZrO_2 with Boarate Additives,'' J. Am. Ceram. Soc., (submitted) (1982).

4. Patents

a. ''Low Temperature Densification of PZT Ceramics,'' by Relva C. Buchanan and Dale E. Wittmer, US Patent #4,283,228, August, 1981.

b. ''Low Temperature Densification of Zirconia Ceramics,'' by Relva C. Buchanan, H. Dale DeFord, and Anup Sircar, US Patent # 4,303,447, December 1, 1981.